

FRACTAL CHARACTERIZATION OF SILTY BEDS/LAMINAE AND ITS IMPLICATIONS FOR THE PREDICTION OF SHALE OIL RESERVOIRS IN QINGSHANKOU FORMATION OF NORTHERN SONGLIAO BASIN, NORTHEAST CHINA

BO LIU^{*,†,‡} LIANG JIN^{*} and CAIZHI HU^{*}

**Institute of Unconventional Oil and Gas*

State Key Laboratory Cultivation Base

Northeast Petroleum University, Daqing 163318, P. R. China

*†State Key Laboratory of Oil and Gas Reservoir Geology and Exploitation
Chengdu University of Technology, Chengdu 610051, P. R. China*

‡liubo@nepu.edu.cn

Received July 15, 2018

Accepted August 25, 2018

Published November 14, 2018

Abstract

Cretaceous Qingshankou Formation (K_2qn) in the Songliao Basin, the largest petroliferous basin in East China, has favorable geological conditions for the shale oil reservoir. Although the first member of Qingshankou formation (K_2qn^1) has the maximum value of the organic matter content (total organic carbon (TOC)) comparing with other members, most of the layers are less than 1 cm. This limits the application of surface seismic survey and logging methods. To explore “sweet spots” of the shale oil and to evaluate resource potential, it is of great significance to determine the thickness and distribution of silty beds/laminae in the thick shale system. In this study, the observed data of the outcrops, cores, and thin sections of K_2qn^1 are used to analyze the characteristics of reservoir space in silty laminae. Distribution model of silty beds/laminae

[‡]Corresponding author.

This is an Open Access article published by World Scientific Publishing Company. It is distributed under the terms of the Creative Commons Attribution 4.0 (CC-BY) License. Further distribution of this work is permitted, provided the original work is properly cited.

was established by using fractal method. The results show that the silty beds/laminae have large particle size, poor sorting, and relatively developed reservoir space. The pore sizes in silty laminae vary greatly, and the diameters are mostly larger than 50 nm. The connectivity between pores is good. Although the thickness of single silty bed/laminae mostly ranges from 1 mm to 6 mm, the average layers per meter (layers/m) of silty bed/laminae range from 2 to 64. This contributes the cumulative thickness 2.73–31.79% of the total thickness of the whole shale reservoir. According to the fractal analysis, the silty beds/laminae have the uniform fractal characteristics in the decimeter, centimeter, and millimeter levels. And the fractal dimension keeps the scale invariance. The layers and thickness of the thin silty laminae, calculated from Number–Size (NS) fractal model, are in good agreement with observations. This indicates that the fractal-based NS model is an effective method to estimate the parameters of the silty laminae, such as layer number, cumulative thickness, and the ratio of sand to formation. This method provides a reliable reference for the “sweet spot” exploration.

Keywords: Fractal Dimension; Number–Size; Silty Beds/Laminae; Qingshankou Shale; Songliao Basin.

1. INTRODUCTION

Shale systems have obvious heterogeneities in mineralogical and structural characteristics. The argillaceous sedimentation usually has a large thickness and consists of silty beds or widely developed laminae.^{1,2} Interested bed, such as silty bed, is defined as a layer of sedimentary rocks or sediments that are bounded by bedding interfaces, and the thickness of the bed ranges from a few millimeters to tens of meters.³ Among these beds, the lamina is the smallest megascopic layer in a sedimentary sequence, which is usually measured in mm. In general, the lamina is usually considered as a thin bed with thickness less than 1 cm.^{3,4} The silty lamina in shale systems is usually deposited in a relative low-energy hydrodynamic conditions,^{1,4} such as the eolian flow, sediment gravity flow or weak reworking of bottom flows.^{2,5,6} Silty laminae are further classified into several types, such as silty–clayey couplets, wavy–lenticular silty or parallel laminae, massive shale beds, etc.^{5,6}

Silty beds/laminae are discovered in all typical petroliferous shale systems in the world, such as the Mississippian Barnett Shale in northern Texas,⁷ Lower Devonian Ohio Shale in northwest Appalachian Basin,⁸ Lower Jurassic Haynesville Shale in east Texas and west Louisiana,⁹ Cretaceous shale in Green River Basin,¹⁰ Triassic Zhangjiatan Shale in Ordos Basin,¹¹ and Permian Lucaogou Shale in Santanghu Basin.¹² Previous studies have shown that the reservoir properties, gas bearing capacity, and fracturing properties of shale systems are closely related to the silty beds/laminae in shale.^{2,6} The silty beds/laminae, which have

obviously better properties than the adjacent sections of shale, are not only major reservoir spaces in shale formations, but also the significant migration pathway during the shale gas gathering.^{11,12} In addition, the mechanical properties of formations change with the increasing brittleness of shale strata due to the presence of silty beds/laminae.¹³ This feature is favorable for the development and preservation of fractures.¹⁴ Generally, shale systems that have thick and dense silty beds/laminae usually have large production potential for shale gas.⁸ Although the distinguished feature of silty beds appealed lots of recent studies on their controlling effects on the generation and accumulation of shale gas,^{11,15,16} there are no reported researches on the distribution of silty laminae in shale systems due to the limited thickness (in mm).

Songliao Basin is the largest petroliferous basin in east China. Studies indicated that the shale systems of the Cretaceous Qingshankou Formation (K_2qn) in Songliao Basin have favorable geological conditions for the formation of shale oil.¹⁷ The first member of the Cretaceous Qingshankou Formation (K_2qn^1) has the highest organic matter content in Songliao Basin. The average total organic carbon (TOC) content is over 2%. The vitrinite reflectance (R_o) is between 0.5% and 1.1%, and the peak temperature of pyrolysis (T_{max}) ranges from 430°C to 450°C. These parameters indicate that the shale formations in K_2qn^1 are in low-mature to mature stage and are currently generating a large quantity of oil.¹⁷ Core observations showed that there are widely developed silty beds/laminae in the Qingshankou shale formations. Most of these silty

beds/laminae are less than 1 cm. There are very limited silty beds above 10 cm. Thus, the silty laminae with thickness less than 1 cm play an essential role in the formation, accumulation, and also the development and potential evaluation of shale oil. However, the state-of-the-art geophysical method, such as seismic survey and borehole logs cannot reach the resolution less than 10 cm.^{11,16,18,19} This limits the identification of the silty beds/laminae. Therefore, it is of great significance for the assessment and exploration of shale oil resources to develop an effective approach to study the characteristics of these silty beds/laminae, including the vertical distribution feature, cumulative number of layers, and cumulative thickness.

Fractal method is usually used to study patterns and features that have no characteristic length but are of self-similarity.²⁰ It has been widely applied in geological studies such as sedimentary system, sequence stratigraphy, fault system, particle size analysis, pore distribution, and seepage flow characteristics.^{21–26} The fractal method aims to estimate the fractal dimension and analyze the relationship between fractal dimension and other parameters. Several models have been developed to calculate fractal dimension according to different subjects of interest. Studies on the thicknesses of stratified geological objects such as sedimentary strata suggested that the distribution of the thicknesses of such stratum has an exponential feature, and their fractal characteristics can be characterized by the *Number–Size* (NS) model.^{27–29}

In this study, sections of Qingshankou shale formations in Gulong Sag of northern Songliao Basin are selected to analyze the characteristics of silty beds/laminae. The thicknesses of various silty beds/laminae in the shale system are measured, and the thickness distribution is compared with that obtained from the outcrops and boreholes of this shale system. Finally, the distribution model for silty beds/laminae in Qingshankou shale formations is developed based on fractal method.

2. GEOLOGICAL SETTING

Songliao Basin, located in the provinces of Heilongjiang, Jilin and Liaoning in China, is a large sedimentary basin with a total area of about 260,000 km² and is surrounded by Xing'an Mountains and Changbai Mountains. The basin has a dual structure of fault-depression, and consists of both the Jurassic fault depression and post-Jurassic

depression. In Jurassic and Cretaceous at about 70 Ma, Songliao Basin was a large inland lake basin where a large number of animals and plants grew. During Cenozoic, the basin entered the shrinking stage as the crust uplifted, forming into the current terrain feature of an endless plain.

The Qingshankou Formation is a depression whose sedimentary period was during the first flooding of Songliao Basin. It is characterized by warm and humid lacustrine facies. Qingshankou Formation is divided into first, second, and third members from bottom to top. This study focuses on the first member. During the sedimentary period of the first member of Qingshankou Formation, massive water ingress occurred due to continuous subsidence of crust in early stage, which created a large lacustrine basin. The lithology in the first member of Qingshankou Formation is mainly black mudstone, mixed with gray siltstone and a small amount of gray ostracoda limestone, gray fine sandstone, ostracoda mudstone, etc. There are also plentiful fossils of nearly 20 categories and more than 200 species, which are primarily ostracoda and a small amount of plant debris and fish fossil fragments. The development of pyrite nodules indicates a strong anoxic environment in the first member of Qingshankou Formation.

The cores selected for measurements in this study are all located in the Gulong Sag which is located to the west of the Central Depression of Songliao Basin and covers an area of about 3700 km² (Fig. 1). Gulong Sag is a deep-water depression in a long geological period, and is the most important hydrocarbon generation sag in the basin. The dip angle of the depression stratum changes mildly, and the tectonic structure pattern remains similar from deep to shallow stratum with good succession, presenting a uniclinal structure of high elevation in northwest and low elevation in southeast.

The Niaohexiang section is located approximately in Baishi quarry area in the north of Binxian and at the south bank of Songhua River, and the outcrop continuously appears along the Songhua River. The latitude and longitude coordinates of the section are 45°55'2.9"N, 127°27'50.4"E. The altitude of rock is nearly horizontal, which is 126°∠16°. The profile strata stably extend in lateral direction, and it can be continuously traced along the key layer. The lithology changes little from bottom to surface, and is gray–green mudstone and argillaceous siltstone of the upper part of the first member of Qingshankou Formation, which are also

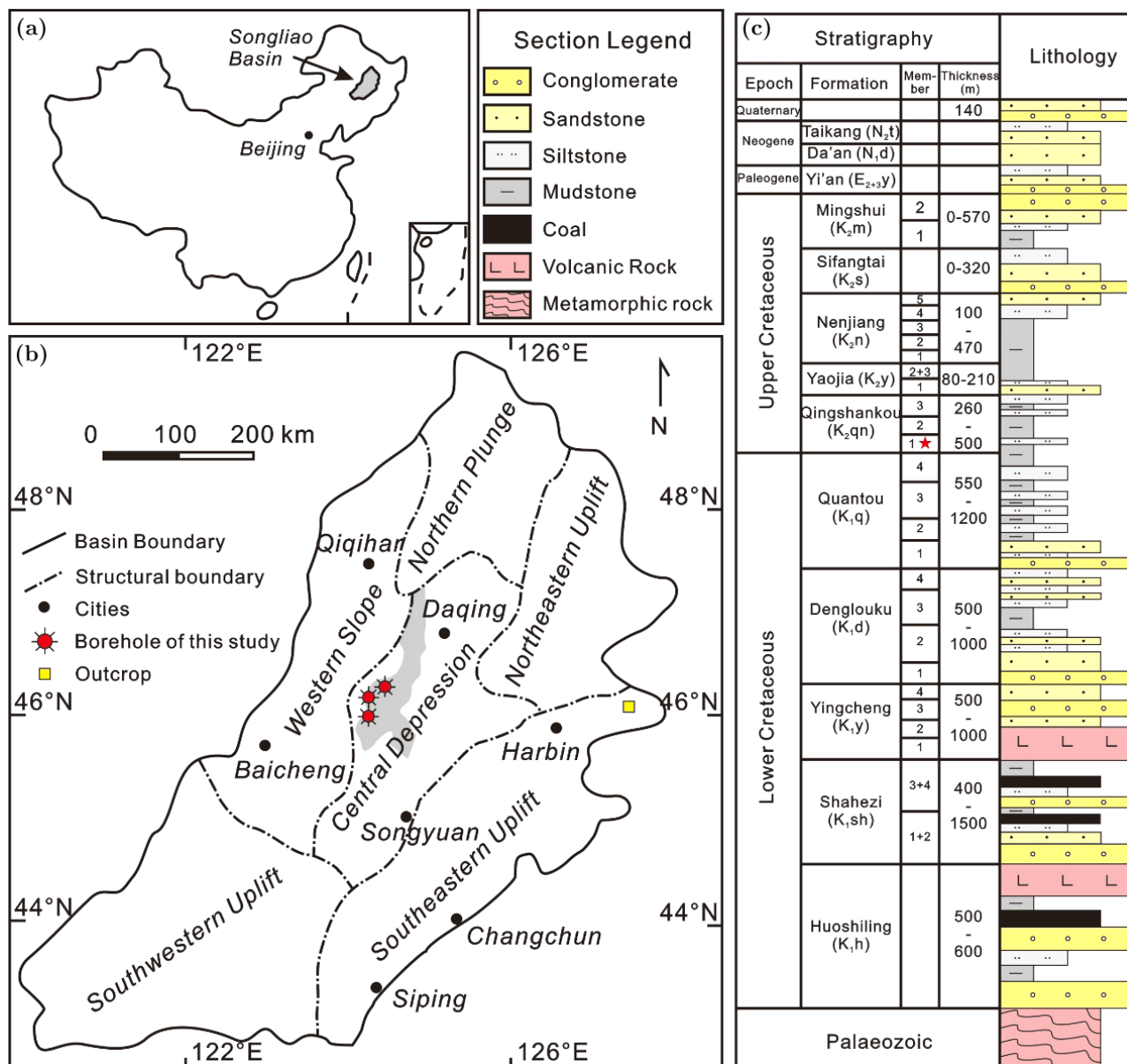


Fig. 1 (a) Location of the Songliao Basin; (b) Central Depression, locations of cores and the outcrop section; (c) general lithologic stratigraphy; gray shadow in (b) indicates the study area of Gulong Sag; red star in (c) indicates the study section in first member of Qingshankou Formation.

interbedded with several layers of shell limestone, dolomite nodules, and pyrite nodules.

The outcrop of Hongshishan section is located in the northeast of Binxian depression, and continuously appears along the Songhua River. The starting latitude and longitude coordinates of the section are 45°55'7.7"N, 127°23'20.3"E. The trending angle is 44°, and the altitude of rock is 224°∠38°. The lower part of the section consists of mudstone with colors varying from dark-green to dark-brown and the argillaceous siltstone, while the middle and upper parts of the section include

red or purple mudstones mingled with dark-green argillaceous band.

Based on the characteristics of the ostracoda, the sections of Niaoheixiang and Hongshishan were determined to belong to the Qingshankou Formation, and their outcrop formations are comparable to the formations in the basin, with similar fossils and paleoecological features.^{30,31} The Niaoheixiang section belongs to the upper part of the first member of Qingshankou Formation and contains the *Triangulicypris torsuosus*–*Triangulicypris torsuosus* var. *nota* assemblage. The Hongshishan

section belongs to the lower part of the second member of Qingshankou Formation and contains the *Cypridea dekhoinensis*–*Limnocypridea copiosa* assemblage, the *Nenestheria sp.*, *Cratostracus sp.*, *Dictyestheria sp.*, and fossiliferous strata.³¹

3. METHODOLOGY

Based on the observations of silty beds/laminae developed in two outcrop sections of Qingshankou Formation and the shale cores of three boreholes in first member of Qinghaikou Formation, this study analyzed the geometry, lithological characteristics, mineral composition, reservoir property, and thickness distributions for these silty beds/laminae. Thin section observation method was applied, and the thickness of silty beds/laminae was measured by a ruler with measurement accuracy in mm level.

3.1. Core and Thin Section Microscopy Analyses

The lithology, sedimentary structures and silty laminae structures were observed from thin sections of core samples under microscope, and the quantity and thickness of a single silty laminae were recorded. Thicknesses of thin sections for petrographic observations and fluorescence analysis were 30 μm and 60 μm , respectively. Petrographic observations were performed using a Leica DMLP polarizing microscope with a Leica DFC450 camera system, and fluorescence analysis was made by using a Nikon Eclipse 80i upright biological fluorescence microscope with a light source of a wavelength 330–380 nm.

3.2. Fractal Methods

The NS model that has been widely applied in geological studies is presented as follows²⁰:

$$N(\geq h) = C \times h^{-D}; \quad C > 0, \quad h > 0, \quad D > 0, \quad (1)$$

where h represents the size of geological objects, in this study, h is the thickness of a single silty bed/laminae; $N(\geq h)$ is the number of objects with size greater than or equal to h ; C is a constant and D is the fractal dimension. As shown in Eq. (1) of the NS model, $N(\geq h)$ and h are linearly correlated in double logarithmic coordinate.

Based on the measurements, a series of $N(\geq h)$ values (i.e. number of silty beds/laminae with thickness greater than or equal to h can be obtained

corresponding to various silty beds/laminae thicknesses (h). Using least square method, a straight line can be created to fit $N(\geq h)$ and h in double logarithmic coordinates. If the fitted line is in good agreement with the data of $N(\geq h)$ versus h in double logarithmic coordinates (i.e. correlation between measured $N(\geq h)$ and h is nearly linear in double logarithmic coordinates), the NS model (i.e. Eq. (1)) can be used to describe the relationship between the measured $N(\geq h)$ and h , and the slope of the fitted line is the fractal dimension (D).

The fractal property has scale invariance, implying that the fractal characteristics are invariant during either magnification or reduction within the scale that has fractal property.²⁰ Thus, the $N(\geq h) - h$ relationship for thick silty beds and thin silty laminae is the same, indicating that the fractal dimension D and the constant C in Eq. (1) are invariant. Therefore, using the NS model, the $N(\geq h) - h$ relationship and the fractal dimension D can be obtained based on data of $N(\geq h)$ and h from thick silty beds, and then can be applied to estimate parameters for thin silty laminae, including the cumulative number and thickness of silty laminae, as well as the ratio of the cumulative thickness of the silty laminae to the total thickness of shale. The number $n(h)$ of silty beds/laminae with thickness equals to h can be calculated from the derivative of Eq. (1):

$$n(h) = \frac{dN(> h)}{d(h)} = C \times D \times h^{-D-1}. \quad (2)$$

The cumulative thickness H for silty beds/laminae with thicknesses between a specific thickness value h_s and the maximum thickness h_{max} can be calculated as follows:

$$\begin{aligned} H &= \sum_{h_s}^{h_{\text{max}}} h = \int_{h_s}^{h_{\text{max}}} \frac{d(N \geq h)}{dh} h dh + h_{\text{max}} \\ &= \frac{C \times D}{1 - D} \times h^{-D+1} \Big|_{h_s}^{h_{\text{max}}} + h_{\text{max}}. \end{aligned} \quad (3)$$

4. RESULTS

4.1. Petrology Characteristics

A large number of silty beds/laminae can be observed in the Qingshankou shale, and their thicknesses range from several millimeters to tens of centimeters, and laminae with only a few microns thickness can also be observed under microscope (Fig. 2). Their colors are mostly white or gray,

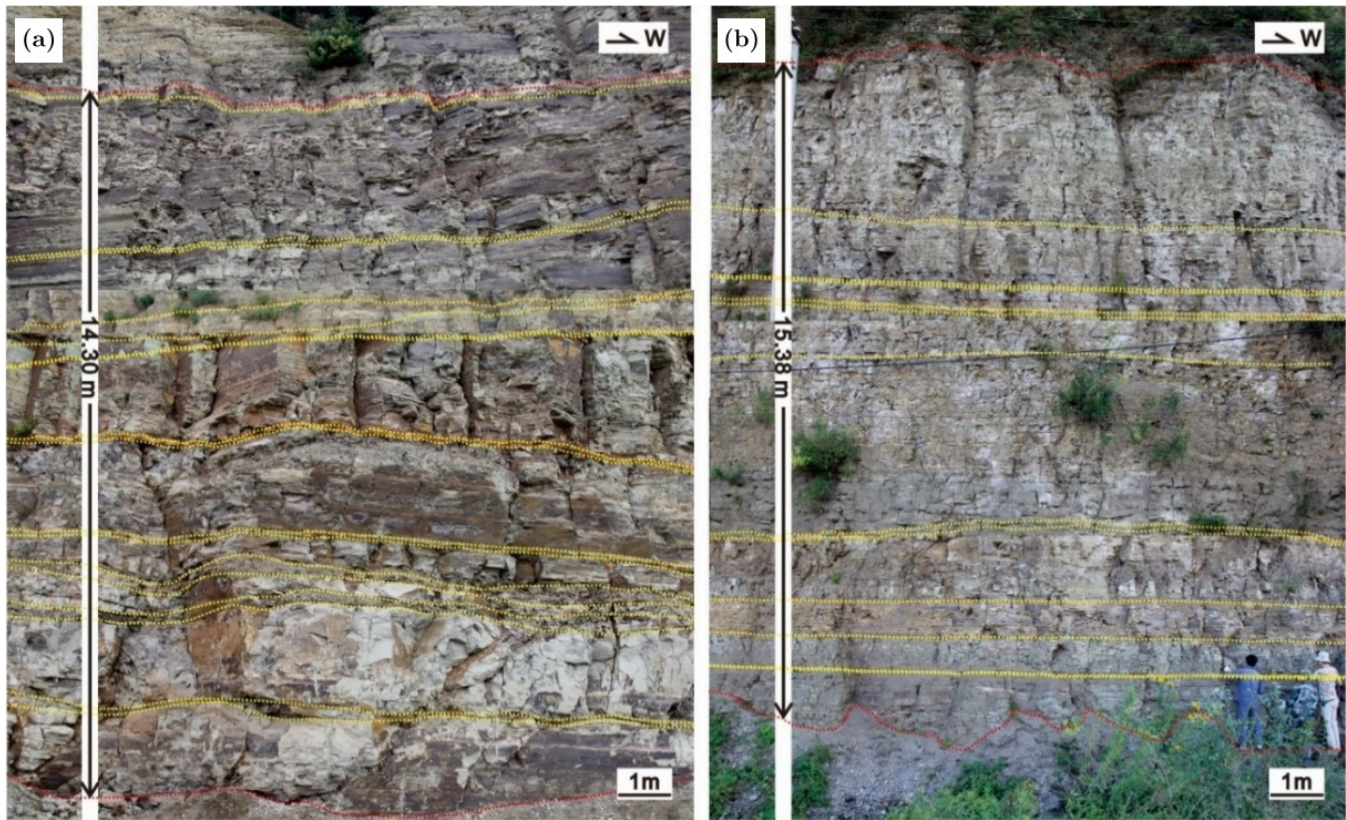


Fig. 2 Qingshankou Shale outcrop profile: (a) Niaohexiang section; (b) Hongshishan section. The red line indicates the top and bottom boundaries of the layer of observation. The yellow dotted line indicates the typical silty beds/laminae. The locations of the sections are indicated in Fig. 1b.

which is quite different from the black clayed laminae. The silty beds/laminae are mainly horizontal or wavy-lenticular, and are interbedded with clayed laminae (Fig. 3). The horizontal beds/laminae are often composed of a single layer or a group of nearly parallel beds/laminae, which can extend to a far distance in horizontal direction, reaching several meters to tens of meters on outcrop. The internal structure of the horizontal beds/laminae is relatively simple, with flat and straight top and bottom interfaces. At bottom interface, sudden changes in the sedimentary tectonics and graded structure are common, while a gradual transition to massive mudstone is common at top interface. The wavy-lenticular silty laminae consist of a series of inter-laminated thin silty laminae and clayed laminae, which usually appear in groups or bundles of about 2–10 layers, with single layer thickness in the range of several millimeters to ten millimeters. Such silty laminae are generally distributed along the lamination direction with relatively poor continuity and certain variability in horizontal direction, and even pinch out or merge with other laminae. Small scale

of interlamination between silty beds/laminae and shale can be observed in some local regions.

The mineral composition and grain sizes are significantly different between silty beds/laminae and clayed laminae. The mineral composition of silty beds/laminae are dominated by quartz, feldspar, and clay minerals, in which the quartz content varies between 21.5% and 41.8%, with an average of 34.5%, the feldspar content varies between 22.3% and 71.2%, with an average of 39.4%, and the clay minerals content, mainly comprised of illite/smectite mixed layer and chlorite, is about 16.5% on average. In addition, calcite, dolomite, pyrite, siderite, biotite, and other minerals can also be observed in silty beds/laminae, and some silty beds/laminae are cemented with calcite. In contrast to the clayed laminae, the silty beds/laminae have larger particle size and poor sorting. The particle sizes of silty beds/laminae are in the range of 4–240 μm , and are mostly between 30 μm and 160 μm , with an average of 40 μm and a median of 34 μm , while the particle sizes of detrital grains of quartz and feldspar in clayed laminae are generally less

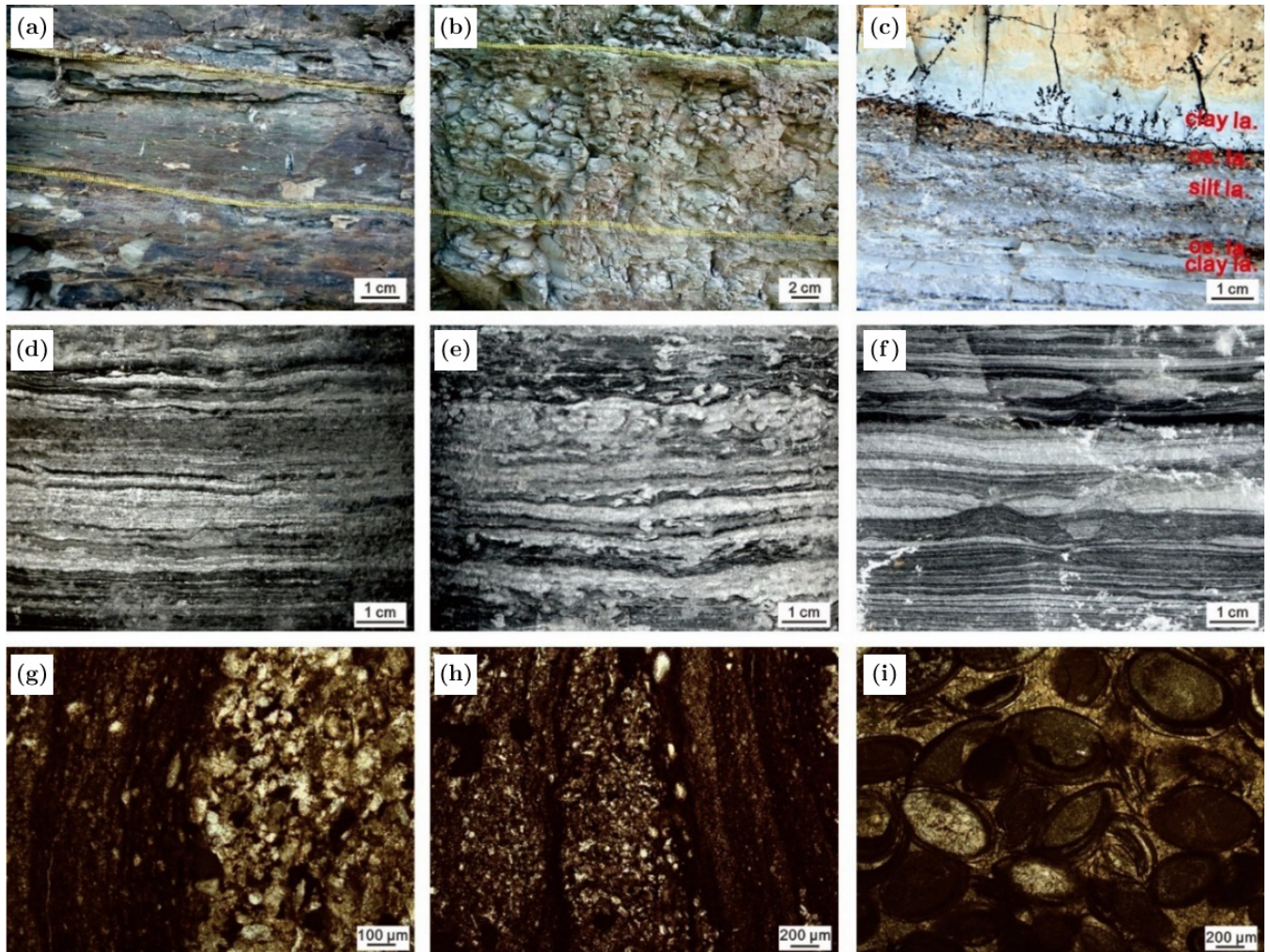


Fig. 3 The petrological characteristics of silty beds/laminae in Qingshankou Shale. (a) and (b) show the silty laminae (yellow dotted-lines) in the sections of Niaohexiang and Hongshishan, respectively; (c) shows the ostracoda laminae in the section of Niaohexiang; (d) shows the horizontal lamination, sampled at the depth of 2090.07 m; (e) shows the turbate lamination, sampled at the depth of 2090.14 m; (f) shows the horizontal and cross-laminations, sampled at the depth of 2206.94 m; (g) and (h) show the mineral composition and grain size of silty and clayed beds/laminae, sampled at the depth of 2202.31 m; (i) shows the microscopic characteristic of ostracoda, sampled at the depth of 2321.61 m. Abbreviations: la.: laminae; os.: ostracoda.

than $10\ \mu\text{m}$, with an average $3.9\ \mu\text{m}$ and a median of $2.8\ \mu\text{m}$.

The development of silty laminae can improve the properties of shale reservoirs.^{12,32} Microscopic observations show that pores are mainly present in silty laminae which are interbedded with clayed laminae which barely have pores developed. There are mainly two types of pores developed in silty beds/laminae: intergranular pores and dissolution pores. The pore sizes vary in a wide range, from a few nanometers to several microns, but are mostly greater than $50\ \text{nm}$. Due to the structural support by the detrital grains, the pores in silty beds/laminae have good connectivity properties. Although the transformation of clay minerals in

clayed laminae may also create some intergranular pores, the pore sizes are only a few nanometers, which leads to poor connectivity.

4.2. Thickness and its Distribution Characteristics

For the Niaohexiang section, the length of the outcrop is $14.31\ \text{m}$ (Fig. 2a), and the altitude of rock is nearly horizontal. The profile strata stably extend in lateral direction, and can be continuously traced along the key layer. Observations indicate that the thicknesses of silty beds/laminae have obvious heterogeneities (Fig. 2a). The number of silty beds/laminae with single layer thickness

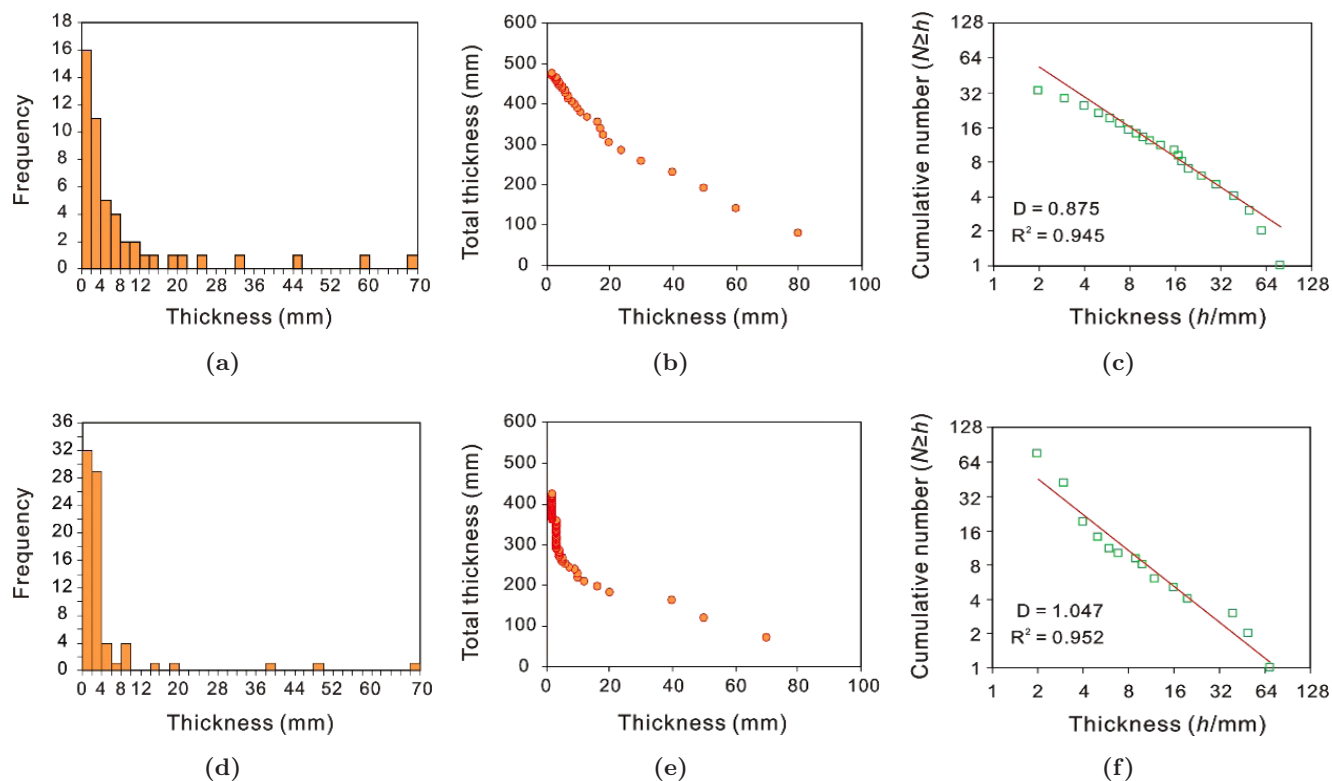


Fig. 4 (a) and (d): the histograms for thickness of silty beds/laminae in outcrop; (b) and (e): single layer thickness versus total thickness; (c) and (f): cumulative number versus single layer thickness. (a)–(c) are for Niaohexiang section; (d)–(f) are for Hongshishan section.

greater than or equal to 2 mm is 33, in which the single layer thickness ranges in 2–6 mm and the cumulative thickness is 476 mm, accounting for 3.32% of the total thickness of the shale. The average layers per meter (layers/m) of silty bed/laminae vary between 1 and 2 layers/m, with an average of 2 layers/m and a maximum of 6 layers/m (Fig. 4).

For the Hongshishan section, the length of the outcrop is 14 m (Fig. 2b), and the number of silty beds/laminae with single layer thickness greater than or equal to 2 mm is 76, in which the single layer thickness ranges in 2–4 mm and the cumulative thickness is 420 mm, accounting for 2.73% of the total thickness of the shale. The average layers per meter (layers/m) of silty bed/laminae vary between 3 and 4 layers/m, with a minimum of 2 layers/m, a maximum of 6 layers/m and an average of 5 layers/m. The cumulative thickness of silty beds/laminae within 1 m thickness of shale formation is 8–12 mm, with a minimum of 6 mm, a maximum of 23 mm and an average of 13 mm (Fig. 4).

The three boreholes (i.e. Y1, Y2 and Y3) for core observations are located at the Western Slope of Gulong Sag (Fig. 1b). Y1 is a continuous coring

well, and the lithology is mainly black mudstone and a small amount of ostracoda. The total number of silty beds/laminae is 1022 in the first member of Qingshankou Formation, and the cumulative thickness is 8.56 m, accounting for 7.62% of the total thickness of the observed shale section. The single layer thickness of the silty beds/laminae is between 1 mm and 6 mm, and the development frequency is about 9 layers/m. In Y2, the lithology is primarily black mudstone with a small amount of silt and ostracoda. The total number of silty beds/laminae is 1208, and the cumulative thickness is 15.49 m, accounting for 19.3% of the total thickness of the observed shale section. The single layer thickness of the silty beds/laminae is between 1 mm and 4 mm, and the development frequency is about 15 layers/m. In Y3, the lithology is mainly black mudstone with a small amount of silt and ostracoda. The total number of silty beds/laminae is 1418, and the cumulative thickness is 7.07 m, accounting for 31.79% of the total thickness of the observed shale section. The single layer thickness of the silty beds/laminae is between 1 mm and 3 mm, and the development frequency is about 64 layers/m.

5. DISCUSSION

5.1. Fractal Characteristics

Based on the measurements at the two sections of Niaohexiang and Hongshishan and core observations at three boreholes in Gulong Sag, the observed number (N) of silty beds/laminae with thickness greater than or equal to h was plotted against the silty beds/laminae single layer thickness h in double logarithmic coordinates (e.g. Fig. 4c), which clearly show linear correlation throughout different measurement scales (i.e. decimeters, centimeters, and millimeters) at all the observation locations (Figs. 4c, 4f and 5d–5f). These data sets present little deviation especially on both sides of the curvature, due to the limitation of statistics resolution and the boundary effect. It is necessary to define two truncations on both sides to fit the best power law distribution. Thus, the fractal-based NS model can be applied for the studies on silty beds/laminae, and the fractal dimension can be calculated. The fractal dimension for silty beds/laminae in Niaohexiang and Hongshishan section is calculated to be 0.875 and 1.047, respectively, and the correlation coefficient is 0.945 and 0.952, respectively. The

fractal dimension for silty beds/laminae of the first member of Qingshankou Formation at Y1, Y2, and Y3 is 1.007, 0.957, and 1.098, respectively, and the correlation coefficients are all over 98%.

5.2. Prediction Model for Silty Beds/Laminae

Although the characteristics of silty beds/laminae can be directly obtained by core observations, the number of coring sections in the study area is usually insufficient and direct observation can be costly and time-consuming. Thus, fractal models can be more efficient in predicting the properties of silty beds/laminae based on core data. In this study, the accuracy of the fractal model for predicting the distributions of silty beds/laminae was assessed by comparing predicted and observed results at Y3. Only the data for thick silty beds/laminae with single layer thickness greater than or equal to 0.1 m were used to establish the NS prediction model, since the maximum accuracy for logging analysis is 0.1 m.^{33,34} The observed number (N) of silty beds/laminae with thickness greater than or equal to h versus the silty beds/laminae

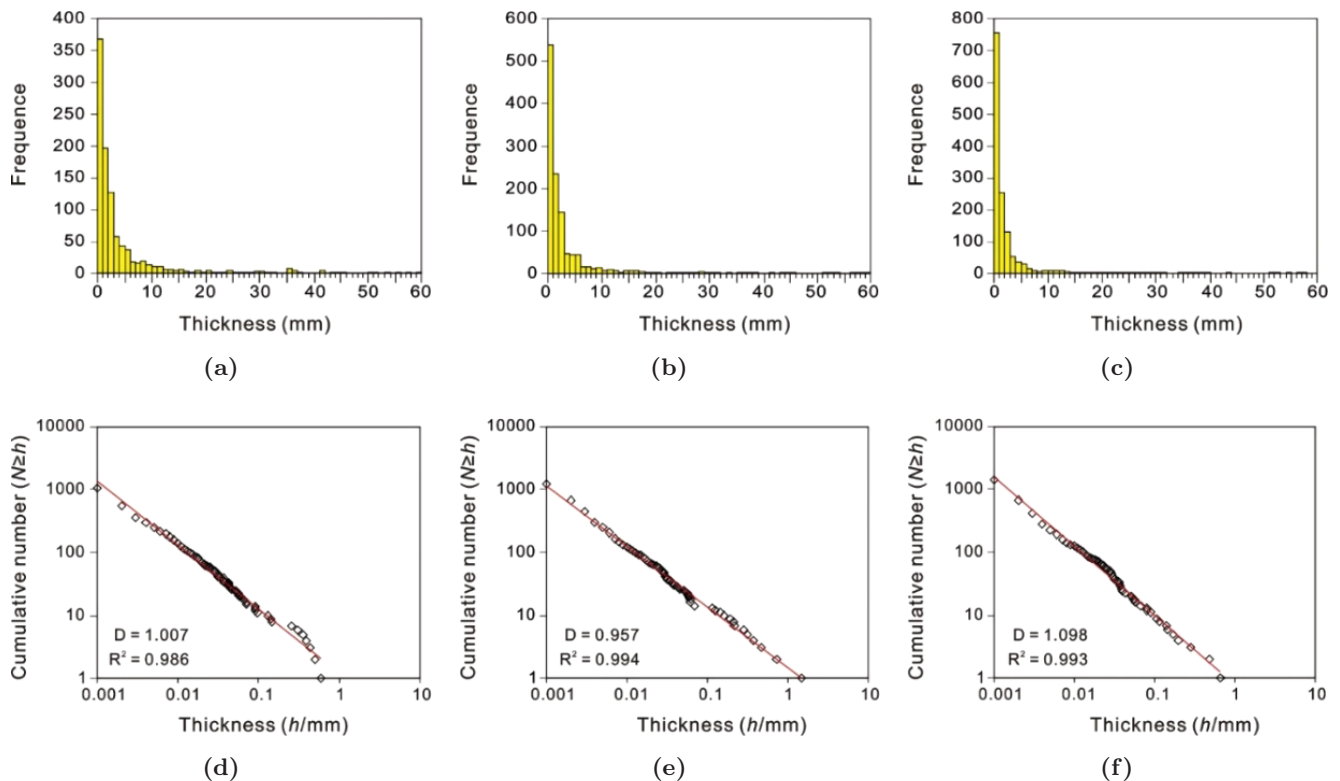


Fig. 5 (a)–(c): histograms for thickness of silty beds/laminae from different boreholes (i.e. Y1, Y2, Y3) in the study area; (d)–(f): cumulative number versus single layer thickness. (a) and (d) are for Y1; (b) and (e) are for Y2; (c) and (f) are for Y3.

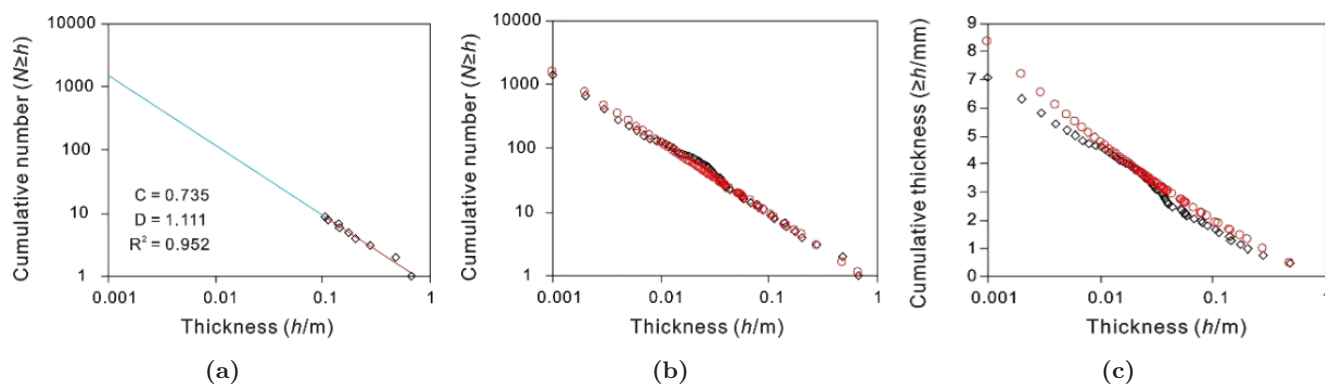


Fig. 6 (a) Cumulative number versus single layer thickness for silty beds that are thicker than 0.1 m in Y3; (b) and (c): comparison between predicted (red circle) and measured values (black diamond) for silty beds/laminae in Y3.

thicknesses (h) that are above 0.1 m was firstly plotted in double logarithmic coordinates (Fig. 6a), and a straight line that represents Eq. (1) of NS model was obtained using least square method to fit the data of $N(\geq h)$ and h . Thus, the NS model for predicting silty beds/laminae distributions in Y3 was established based on data of thick silty beds with single layer thickness above 0.1 m, and the fractal dimension D and constant C in Eq. (1) of the NS model were calculated to be 1.111 and 0.735, respectively, and the correlation coefficient R^2 for the data of $N(\geq h)$ and h is 0.953. The cumulative thickness H between a specific thickness h_S and the maximum thickness h_{\max} can also be obtained from Eq. (3).

Using this NS model (i.e. $C = 0.735$ and $D = 1.111$ for Eq. (1)) which is based on data of thick silty beds with single layer thickness above 0.1 m, the cumulative number of layers and cumulative thickness of silty beds/laminae in a series of thickness ranges in Y3 were predicted and compared with observations (Figs. 6b and 6c). In Y3, the observed and predicted cumulative numbers of silty beds/laminae are 1418 and 1582, respectively, indicating a prediction error of approximately 11.57%. The observed and predicted cumulative thicknesses of silty beds/laminae in Y3 are 7.071 m and 8.341 m, respectively, indicating a prediction error of approximately 17.96%. The predicted cumulative number and cumulative thickness of silty beds/laminae are in good agreement with observations.

Therefore, the NS model based on fractal theory breaks through the limitation of insufficient resolution of seismic and logging techniques in the silty beds/laminae. The application of the NS model can effectively predict the cumulative number and thickness of silty beds/laminae that have fractal

properties in shale systems. It is very helpful for effectively characterizing and predicting the distribution of shale oil “sweet spot” in different scales.

6. CONCLUSION

(1) The silty beds/laminae are comprised of quartz, feldspar, and clay minerals (e.g. illite/smectite mixed layer and chlorite) whose contents are 34.5%, 39.4%, and 16.5%, respectively. The detrital grain size in silty laminae is $40 \mu\text{m}$ on average, and the median size is $34 \mu\text{m}$, while the detrital grain size in clayed laminae is generally less than $10 \mu\text{m}$, with an average of $3.9 \mu\text{m}$ and a median of $2.8 \mu\text{m}$. The detrital grain size in silty laminae is generally larger than that in clayed laminae.

(2) Silty beds/laminae are widely developed in shale systems of Qingshankou Formation in Songliao Basin. The single layer thicknesses of silty beds/laminae vary in the range of 1–6 mm, and the development frequency is about 2–64 layers/m. The cumulative thickness of silty beds/laminae accounts for 2.73–31.79% of the total thickness of shale.

(3) The thickness distribution of silty beds/laminae developed in shale systems of the first member of Qingshankou Formation in Songliao Basin has obvious fractal characteristics, implying the cumulative number (N) of silty beds/laminae with thickness greater than or equal to h is linearly correlated with the silty beds/laminae single layer thickness h , and the fractal characteristics remain invariant with respect to different thickness ranges. Using the NS model, the predicted cumulative number and cumulative thickness of the silty beds/laminae are in good agreement with observations. The fractal-based NS model is an effective method for predicting the parameters, such as

layers, cumulative thickness and the ratio of sand to formation thickness of silty laminae. This method can provide reliable reference for the “sweet spot” exploration.

ACKNOWLEDGMENTS

This study was supported by Open Fund (PLC201 80402) of the State Key Laboratory of Oil and Gas Reservoir Geology and Exploitation (Chengdu University of Technology) and the National Natural Science Foundation of China (Nos. 41472125, U1562214). Thanks also to the University Nursing Program for Young Scholars with Creative Talents in Heilongjiang Province (UNPYSCT-2015077, QC2015043), and the National Basic Research Program of China (2016ZX05003-002) for financial support. Samples were provided by the Daqing Oil Company in China.

REFERENCES

1. A. E. S. Kemp, Laminated sediments as palaeo-indicators, in *Palaeoclimatology and Palaeoceanography from Laminated Sediments* (Geological Society Special Publications, London, 1996), pp. vii–xii.
2. N. R. O'Brien, Shale lamination and sedimentary processes, in *Palaeoclimatology and Palaeoceanography from Laminated Sediments* (Geological Society Special Publications, London, 1996), pp. 23–36.
3. C. V. Campbell, Lamina, laminaset, bed and bedset, *Sedimentology* **8** (1967) 7–26.
4. P. E. Potter, J. B. Maynard and P. J. Depetris, *Mud and Mudstones: Introduction and Overview* (Springer Science & Business Media, 2005), p. 248.
5. D. L. Carey and D. C. Roy, Deposition of laminated shale: A field and experimental study, *Geo-Marine Lett.* **5** (1985) 3–9.
6. J. Schieber, Significance of styles of epicontinental shale sedimentation in the belt basin, mid-proterozoic of Montana, USA, *Sediment. Geol.* **69** (1990) 297–312.
7. R. M. Slatt and N. R. O'Brien, Pore types in the Barnett and Woodford gas shales: Contribution to understanding gas storage and migration pathways in fine-grained rocks, *Am. Assoc. Pet. Geol. Bull.* **95** (2011) 2017–2030.
8. R. F. Broadhead, R. C. Kepferle and P. E. Potter, Stratigraphic and sedimentologic controls of gas in shale — Example from Upper Devonian of northern Ohio, *Am. Assoc. Pet. Geol. Bull.* **66** (1982) 10–27.
9. U. Hammes, H. S. Hamlin and T. E. Ewing, Geologic analysis of the upper jurassic haynesville shale in east Texas and west Louisiana, *Am. Assoc. Pet. Geol. Bull.* **95** (2011) 1643–1666.
10. J. Frederick Sarg *et al.*, Lithofacies, stable isotopic composition, and stratigraphic evolution of microbial and associated carbonates, Green River Formation (Eocene), Piceance Basin, Colorado, *Am. Assoc. Pet. Geol. Bull.* **97** (2013) 1937–1966.
11. Y. Lei *et al.*, Characteristics of silty laminae in Zhangjiatan shale of southeastern Ordos Basin, China: Implications for shale gas formation, *Am. Assoc. Pet. Geol. Bull.* **99** (2015) 661–687.
12. B. Liu *et al.*, Petrologic characteristics and genetic model of lacustrine lamellar fine-grained rock and its significance for shale oil exploration: A case study of Permian Lucaogou Formation in Malang sag, Santanghu Basin, NW China, *Pet. Explor. Dev.* **42** (2015) 656–666.
13. S. E. Laubach, J. E. Olson and M. R. Cross, Mechanical and fracture stratigraphy, *Am. Assoc. Pet. Geol. Bull.* **93** (2009) 1413–1426.
14. G. G. Lash and T. Engelder, An analysis of horizontal microcracking during catagenesis: Example from the Catskill delta complex, *Am. Assoc. Pet. Geol. Bull.* **89** (2005) 1433–1449.
15. C. Han *et al.*, The lithofacies and reservoir characteristics of the Upper Ordovician and Lower Silurian black shale in the Southern Sichuan Basin and its periphery, China, *Mar. Pet. Geol.* **75** (2016) 181–191.
16. P. Wang *et al.*, Lithofacies classification and its effect on pore structure of the Cambrian marine shale in the Upper Yangtze platform, South China: Evidence from FE-SEM and gas adsorption analysis, *J. Pet. Sci. Eng.* **156** (2017) 307–321.
17. C. Liu *et al.*, Enrichment and distribution of shale oil in the Cretaceous Qingshankou Formation, Songliao Basin, Northeast China, *Mar. Pet. Geol.* **86** (2017) 751–770.
18. H. Wang, G. Tao and X. Shang, A method to determine the azimuth angle of interface outside of borehole by monopole borehole acoustic reflections, *J. Pet. Sci. Eng.* **133** (2015) 304–312.
19. H. Li and H. Wang, Investigation of eccentricity effects and depth of investigation of azimuthal resistivity LWD tools using 3D finite difference method, *J. Pet. Sci. Eng.* **143** (2016) 211–225.
20. B. Mandelbrot, How long is the coast of Britain? Statistical self-similarity and fractional dimension, *Science* **156** (1967) 636–638.
21. C. E. Krohn, Fractal measurements of sandstones, shales, and carbonates, *J. Geophys. Res.* **93** (1988) 3297.
22. B. D. M. Gauthier and S. D. Lake, Probabilistic modeling of faults below the limit of seismic resolution in Pelican field, North Sea, offshore United Kingdom, *Am. Assoc. Pet. Geol. Bull.* **77** (1993) 761–777.
23. T. Dutta and S. Tarafdar, Fractal pore structure of sedimentary rocks: Simulation by ballistic

- deposition, *J. Geophys. Res. Solid Earth* **108** (2003) 1–6.
24. F. Storti, A. Billi and F. Salvini, Particle size distributions in natural carbonate fault rocks: Insights for non-self-similar cataclasis, *Earth Planet. Sci. Lett.* **206** (2003) 173–186.
 25. A. Billi and F. Storti, Fractal distribution of particle size in carbonate cataclastic rocks from the core of a regional strike-slip fault zone, *Tectonophysics* **384** (2004) 115–128.
 26. W. Schlager, Fractal nature of stratigraphic sequences, *Geology* **32** (2004) 185–188.
 27. R. J. Bailey and D. G. Smith, Quantitative evidence for the fractal nature of the stratigraphic record: Results and implications, *Proc. Geol. Assoc.* **116** (2005) 129–138.
 28. P. Zhao *et al.*, Investigation on the pore structure and multifractal characteristics of tight oil reservoirs using NMR measurements: Permian Lucaogou Formation in Jimusaer Sag, Junggar Basin, *Mar. Pet. Geol.* **86** (2017) 1067–1081.
 29. Q. Wang *et al.*, The fractal relationship between ore-body tonnage and thickness, *J. Geochem. Explor.* **122** (2012) 4–8.
 30. Z. Zhang *et al.*, Ostracod biostratigraphy of the late Cretaceous Qingshankou Formation in the Songliao Basin, *Acta Geol. Sin.* **81** (2007) 727–738 (in Chinese).
 31. W. Si *et al.*, Ostracode stratigraphy and palaeoenvironment of the Cretaceous Qingshankou Formation in East Songliao Basin, *Acta Geol. Sin.* **84** (2010) 1389–1400 (in Chinese).
 32. X. Ge *et al.*, Investigation of organic-related pores in unconventional reservoir and its quantitative evaluation, *Energy Fuels* **30** (2016) 4699–4709.
 33. H. Li and M. Fehler, The wavefield of acoustic logging in a cased hole with a single casing — Part I: A monopole tool, *Geophys. J. Int.* **212** (2018) 612–626.
 34. H. Li and M. Fehler, The wavefield of acoustic logging in a cased hole with a single casing — Part II: A dipole tool, *Geophys. J. Int.* **212** (2018) 1412–1428.